Nanoindentation and nano-scratch studies on cement paste containing short MWCNTs

Salim Barbhuiya[1], Bibhuti Bhusan Das[2]

[1] Department of Engineering and Construction, University of East London, United Kingdom

[2] Civil Engineering Department, National Institute of Technology Surathkal, India

Email: s.barbhuiya@uel.ac.uk

Abstract

Carbon nanotubes (CNTs) are an attractive reinforcement material for several composites. This is due to their inherently high tensile strength and high modulus of elasticity. This study looked at the nanomechanical characteristics of cement paste with and without short multi-walled carbon nanotubes (MWCNTs). The objective behind studying the nanomechanical properties of cement paste is to better understand the fundamental behaviour of cement at the nanoscale level. Cement paste is a complex material that consists of various phases, including cement hydrates, un-hydrated cement particles, and porosity. By studying the mechanical properties of cement paste at the nanoscale, researchers can gain insights into the mechanisms that govern the behaviour of this material. Following earlier tests, the amount of MWCNTs was kept constant (0.30% by weight of cement). Nanomechanical parameters explored include localised Young's modulus and hardness. According to test results, short MWCNTs increased the proportion of high-density calcium silicate hydrate in cement paste. The nanomechanical properties (localised Young's modulus and hardness) of cement paste with short MWCNTs was found to be greater than that of cement paste without MWCNTs. According to nano-scratching experiments the cement matrix with short MWCNTs is substantially more durable than the matrix without them.

Keywords: Nanoindentation; nano-scratch; short multi-walled carbon nanotubes; elastic modulus, hardness

1. Introduction

The brittleness of cement composites is high. The fundamental reason for this is composites' poor tensile strength (Chen et al., 2011). Researchers have tried a range of materials to improve the tensile strength of cement composites (Fischer and Li, 2007; Savastano et al., 2005; Wang et al., 2008). Such materials include glass, steel, carbon and fibres. In the literature, carbon nanotubes (CNTs) have also been employed as a reinforcing material (Chen et al., 2003; Esawia et al., 2009; Lau and Hui, 2002; Lee et al., 2007; Wei et al., 2008; Zhu et al., 2008). These are allotropes of carbon with a cylindrical nanostructure.

SWCNTs (single-walled carbon nanotubes) and MWCNTs (multi-walled carbon nanotubes) are two forms of carbon nanotubes. MWCNTs are composed of nesting graphene arrays, whereas SWCNTs are made of a single sheet of graphene rolling into a long hollow cone. It has been observed that the porosity and pore size distribution decreases when MWCNTs are used in cement composites (Wang et al., 2014). MWCNTs also have a considerable impact on the microstructure of high-performance mortar (Sahranavard et al., 2014).

MWCNTs are said to affect the cement hydration (Li et al., 2015). As MWCNTs provide more calcium silicate hydrate (CSH) gel sites, the use MWCNTs produces a high-strength cement paste with a dense matrix. However, the dispersion of MWCNTs within cementitious composites is a major concern. Nevertheless, a tiny amount of MWCNTs addition to concrete considerably improves their mechanical strength and fracture behaviour (Gillani et al., 2017). The need of proper MWCNTs dispersion in the cement matrix is emphasised even further in this study. MWCNTs come in a variety of lengths. Short MWCNTs have low aspect ratios (150-400), corresponding to 0.5-2 μm lengths and outer diameters ranging from 7 nm to 80 nm, whereas long MWCNTs have high aspect ratios (1000-2000). The distribution of short MWCNTs is much uniform than that of long MWCNTs. This allows them to effectively occupy nanopore space within the cement matrix (Abu Al-Rub et al., 2012).

Hawreen and Bogas (2019) concluded that concrete with functionalised CNTs exhibit similar behaviour to that with pristine CNTs of equal aspect ratio. The dynamic mechanical properties of cementitious composites with different sizes such as thick–long, thick–short, thin–long, thin–short, large inner tall-wall, helical, nickel-coated, graphitised MWCNTs was also analysed by researchers (Wang et al., 2020). The cement pastes with thick–short MWCNTs showed the highest impact toughness with 100.8% increase over the plain cementitious composites, while the samples with thin–long MWCNTs exhibited a 77.7% improvement to impact energy dissipation. In other study, the effect of carbon nanotube purity on properties of cement paste containing 1% MWCNTs by weight of binder was evaluated (Yoo et al., 2018). The effect and mechanism of functionalised MWCNTs on CSH gel was evaluated using Scanning Electron Microscopy with Energy Dispersive X-Ray analysis by Li et al. (2020). The authors concluded that, when preparing cement paste with MWCNTs, these should be combined with functional groups to improve CSH content. The functional groups here refer to the hydrophilic functional groups on the surface of the MWCNTs through chemical reactions such as acidification and oxidation. These hydrophilic functional groups can improve the dispersion degree of the MWCNTs in aqueous solution.

Cui et al. (2017) analysed the effects of 12 types of MWCNTs and dosage levels (0.1–0.8% replacing cement by weight) on mechanical properties. The authors found that short, pristine, large-diameter MWCNTs show the best performance in terms of the strength of cement pastes. The authors also illustrated that MWCNTs with hydroxyl groups show better performance on the strength of cement paste compared to the MWCNTs with carboxyl groups. Hawreen et al. (2018) investigated the effects of different types of carbon nanotubes on mechanical strength, ultrasonic pulse velocity and fracture toughness of cement paste. There was an increase in the flexural strength and fracture energy up to 33% and 65% with the addition of 0.05–0.1% of carbon nanotubes, respectively. Arrechea et al. (2020) prepared MWCNT reinforced cement mortar with three types of carbon nanotube: pristine, carboxylated-functionalised and thiazol-functionalised. The authors used different weight ratios of MWCNTs to produce cement mortars (0.01–0.05% w/w) with polycarboxylate-based super-plasticiser. It was observed that there was an improvement in compressive strength by 5.3% with 0.01% of MWCNTs.

Nanoindentation is a technique for assessing the local mechanical properties of cement-based materials quantitatively (Mondal et al., 2007). It is the latest technology that enables researchers to measure mechanical properties such as modulus and hardness of materials in different shapes, sizes and scales. Most notably, this technique does not need any sample preparation and can measure properties for various materials ranging from hard superalloys to soft biomaterials within seconds making it the fastest technique for such measurements. It is a significant development over regular uniaxial tensile and shear testing methods that take days from samples preparation to final results. In nanoindentation contact between the substrate (the sample) and an indenter with predetermined features and form can be used to ascertain the substrate's elastic and hardness properties. To carry out the experiment more precisely, the 'grid' indentation approach, also known as the 'statistical nanoindentation system' (SNI), has been used by various researchers (Davydov et al., 2011; Sorelli et al., 2008; Vandamme et al., 2010). Nanoscratch tests, on the other hand, are commonly employed in coatings and bulk materials to assess adhesion and wear efficiency in a transparent, flexible and timely manner (Adams et al., 2001; ; Graca et al., 2008; Shen et al., 2006). The ideal amount of MWCNTs in cement composites is 0.08% (Wang et al., 2008). It is estimated that it can be used up to 0.50% (Kumar et al., 2012). This study investigates the nanomechanical characteristics of cement paste with 0.30% (by weight of cement) short MWCNTs.

Nanoindentation and nano-scratch studies are valuable techniques in the characterization of the mechanical properties of materials, particularly at the nanoscale level. These techniques allow for the measurement of key mechanical properties such as hardness, elastic modulus, and friction. When applied to cement paste, these techniques provide a valuable insight into the effect of adding MWCNTs to the material.

The addition of MWCNTs to cement paste has been shown to improve its mechanical properties. However, the mechanism by which this occurs is not fully understood. Nanoindentation studies have been used to investigate the effect of MWCNTs on the hardness and elastic modulus of cement paste. These studies have shown that the addition of MWCNTs increases the hardness and elastic modulus of cement paste, indicating an improvement in its mechanical strength. In addition to nanoindentation studies, nano-scratch studies have also been used to investigate the effect of MWCNTs on the frictional properties of cement paste. These studies have shown that the addition of MWCNTs reduces the coefficient of friction of cement paste, indicating an improvement in its wear resistance.

The significance of these studies lies in the fact that they provide valuable insights into the effect of adding MWCNTs to cement paste, which can be used to develop more effective cement composites. These studies also provide a better understanding of the mechanisms by which MWCNTs improve the mechanical properties of cement paste, which can inform the development of new and improved cement composites.

2. Experimental programme

2.1 Materials

In this experiment, a general-purpose grey Portland Cement was used. Cockburn Cement in Western Australia supplied the cement, which was approved to AS 3972: 2010 for general purpose and mixed cements. Table 1 shows the chemical composition of cement. US Research Nanomaterials, Inc. provided the short MWCNTs used in the investigations. They were made using chemical vapour discharge (CVD). Table 2 lists the characteristics of short MWCNTs. The water used was normal tap water.

Table 1: Chemical composition of cement (oxide %)

SiO_2	20.95
Al_2O_3	4.72
Fe_2O_3	3.00
CaO	62.85
SO_3	2.6
MgO	2.2
Chloride	0.02
Na_2O Equivalent	0.40
LOI	2.0

Table 2: Properties of short MWCNTs

Purity	> 95%
Length	0.5-2 μm
Outside diameter	50-80 nm
Inside diameter	5-15 nm
True density	2.1 g/cm^3
Specific surface area	40 m^2/g

2.2 Sample preparation

The first sample was totally formed of OPC, while the second was made of short MWCNTs (0.30% by wt. of cement). Both cement pastes had a 0.35 water-to-cement ratio. A polycarboxylate-based superplasticiser disperses CNTs effectively while having no influence on hydration time, according to Yazdanbakhsh et al., (2009). According to research, the dispersion process consumes 75% of the polycarboxylate-based superplasticizer (used in MWCNTs samples), while the remaining 25% increases the workability of cement paste (Abu Al-Rub et al., 2012). Therefore, 0.10% and 0.40% (by weight of cement) polycarboxylate-based superplasticizers were added to samples of plain cement paste and cement paste containing short MWCNTs, respectively.

For nanoindentation testing, small cube samples (10×10×10 mm) were made. All cast samples were held for 24 hours in a temperature-controlled curing chamber at a constant temperature of 23(±1)^{0}C before being demoulded. Before being placed in the curing room, the samples were bathed in lime-saturated water. On the 7th, 28th, and 56th days, flexural strength tests were done. After the flexural strength tests, small flat broken fragments were collected for use in the SEM. The materials for nanoindentation testing were ground and polished on the 28th day with a grinder-polisher machine. In four steps, the roughness of 240, 360, 800 and 1200 grit diamond carbide paper was reduced: 52.2, 35.0, 21.8 and 15.3 μm, respectively. After that, the samples were polished using a polycrystalline diamond suspension with different roughness levels: 9, 6, 3, 1, 0.25 and 0.1 μm. Each particle size was polished for 5 minutes with a 20 N applied force, with the exception of the 9 μm, which was polished for 10 minutes.

2.3 Test methods

2.3.1 Nanoindentation

To create local deformation in nanoindentation testing, a controlled force of 1mN was applied to material surfaces. The lower elastic modulus was calculated using well-known equations (Eqs. 2–5) based on elastic contact theory principles (Fischer-Cripps, 2006). Throughout the test, the applied load and associated displacement were continually measured. A typical load-displacement curve was created as a consequence (Fig. 1). The contact stiffness (S), which is determined by the initial slope of the unloading curve, is given by:

$$S = \frac{dP}{dh} \qquad (2)$$

where

P: indentation load

h: indentation depth

A Power Law equation, as illustrated below, fits the beginning portion of the unloading curve:

$$S = \frac{2\beta}{\sqrt{\pi}}\left(\frac{1}{E_r}\right)^{-1}\sqrt{A_c} \qquad (3)$$

The relationship between E_r and modulus of the sample (E) and elastic modulus of the indenter (E_i) is:

$$\frac{1}{E_r} = \frac{1-v^2}{E} + \frac{1-v_i^2}{E_i} \qquad (4)$$

where

v is the Poisson's ratios of sample

v_i is the Poisson's ratios of indenter

E_i =1140G Pa, $v_i = 0.07$ for Berkovich indenter

So, the reduced elastic modulus, E_r is:

$$E_r = \frac{\sqrt{\pi}}{2\beta}\frac{S}{\sqrt{A_c}} \qquad (5)$$

A Berkovich indenter tip and an Agilent Nano Indenter® G200 nanoindentation equipment were employed in this study. Indentation testing on a fused quartz standard specimen yielded the calibrated contact area function. In each study, the loading began when the indenter made contact with the test surface. Before being discharged, the load was held at its maximum value for 30 seconds. Using unloading data for the lower indentation depth (i.e., h_p=300-400 nm), the reduced modulus at the indentation point was determined. The information was gathered from 8 different locations, each with 40 indents (10×4 grid), for a total of 320 indents. The distance between indentations was fixed to 20 µm. After that, a frequency histogram was created utilising statistical analysis of the data.

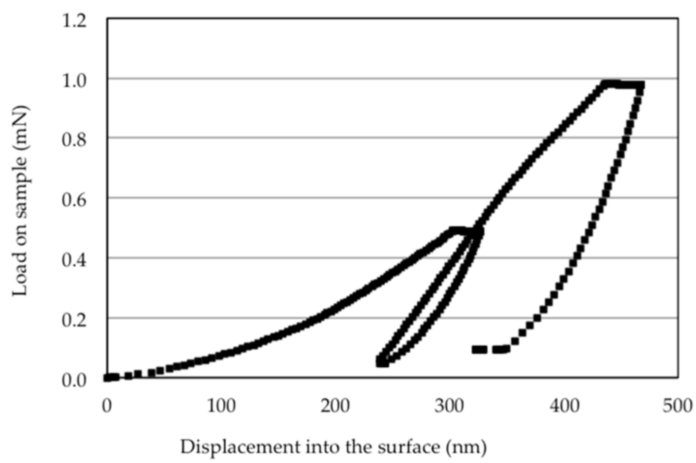

Fig. 1: Typical load-displacement curve

2.3.2 Nano-scratch

The indenter tip made contact with the specimen surface to conduct nano-scratch testing. With a force of 5 N and a displacement rate of 2 m/s, the Berkovich tip was used to perform pre- and post-scratch scans of the surface. 5 spots per metre were scanned in order to gather information. The indentation tip scratched a 100 m length at each target location while scanning the approach and separation zones of the scratch site every 20 metres. A maximum force of 50 mN and a speed of 2 m/s were applied perpendicular to the plane of the sample faces during the scratching process.

3. Results and Discussion

3.1 Nanoindentation

The findings from cement paste with/without short MWCNTs appear to be supported by data obtained from nanoindentation in the literature (Table 3). The elastic modulus of common cement pastes has been divided into five distinct phases (Acker, 2001; Constantinides and Ulm, 2004; Velez et al., 2001). The phases are: porous, low-density CSH, high-density CSH, calcium hydroxide and clinker. The ranges of elastic modulus of these phases are: porous (0–10 GPa), low density CSH (10–25 GPa), high density CSH (25– 35GPa), calcium hydroxide (35– 45GPa) and clinker (> 45 GPa).

Figures 2 and 3 show the elastic modulus frequency graphs for cement pastes with and without short MWCNTs. Values greater than 45 GPa are removed from the charts (which correspond to clinker stages). Both pictures show a wide range of distribution patterns, suggesting that the mechanical behaviour of both cement pastes varies depending on location. Figures 2 and 3 depict the mean peak of the elastic frequency plot for plain cement paste in the low-density CSH gel area (10-25 GPa). The high-density CSH gel area (25-30 GPa) became more apparent when short MWCNTs were added.

Table 3: Values of elastic modulus from literatures (mean ± SD)

Phase	Elastic modulus (GPa)	Reference
Porous	9.2 ± 2.4	Wang et al., 2020
Low-density CSH	19.7 ± 2.5	Wang et al., 2020
	21.7 ± 2.2	Wang et al., 2013
	22.5 ± 5.0	Yoo et al., 2018
High-density CSH	29.4 ± 2.4	Wang et al., 2013
	30.4 ± 2.9	Yoo et al., 2018
	34.2 ± 5.0	Wang et al., 2020
Calcium hydroxide	36.2 ± 3.1	Shen et al., 2006
Clinker	126 ± 24	Graca et al., 2008

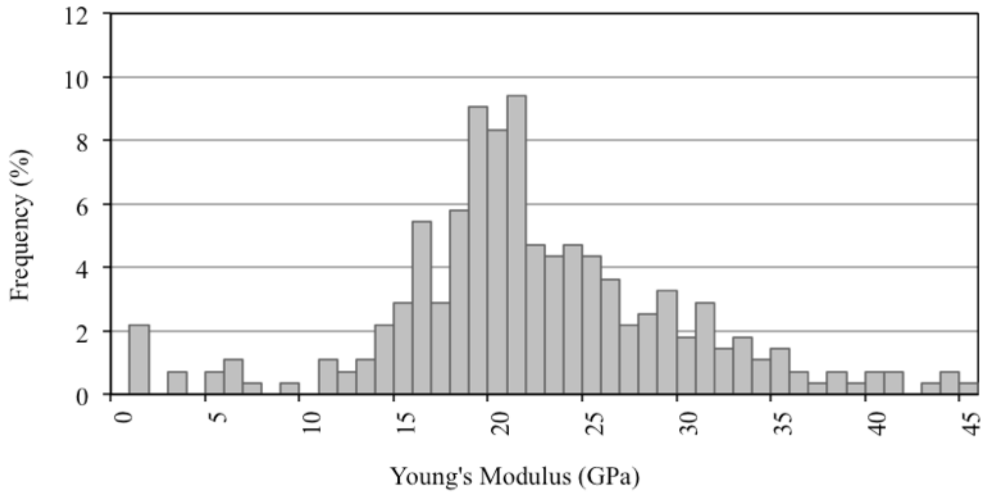

Fig. 2: Probability Frequency Distribution of elastic modulus (plain cement paste)

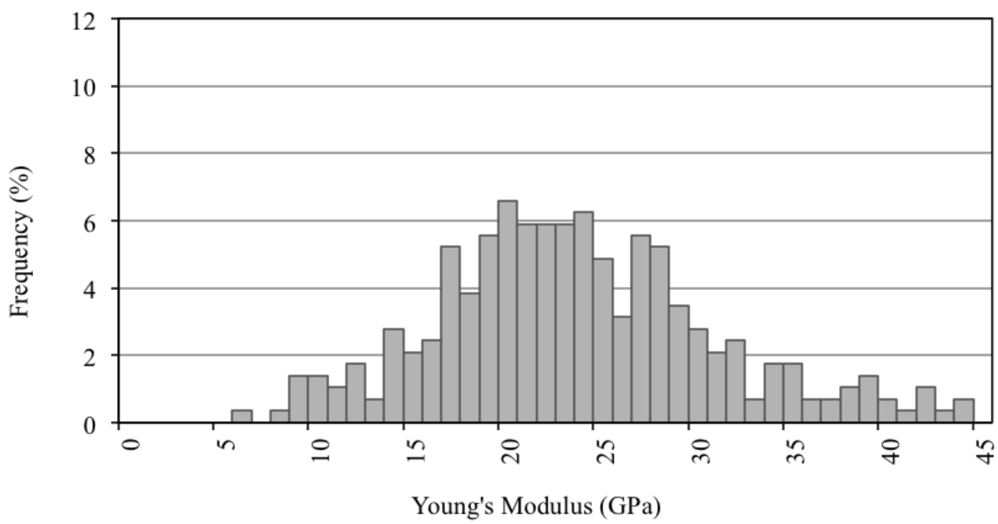

Fig. 3: Probability Frequency Distribution of elastic modulus (cement paste with short MWCNTs)

For eight different samples, Figure 4 shows bar charts of the elastic moduli of cement pastes with and without short MWCNTs. The elastic modulus of each bar is determined by averaging 320 measurements of nanoindentation point modulus. The typical range is 19.5 to 34.0 GPa. When compared to the other samples, the cement paste reinforced with short MWCNTs has a larger elastic modulus, as can be seen in the image, indicating that it is stiffer.

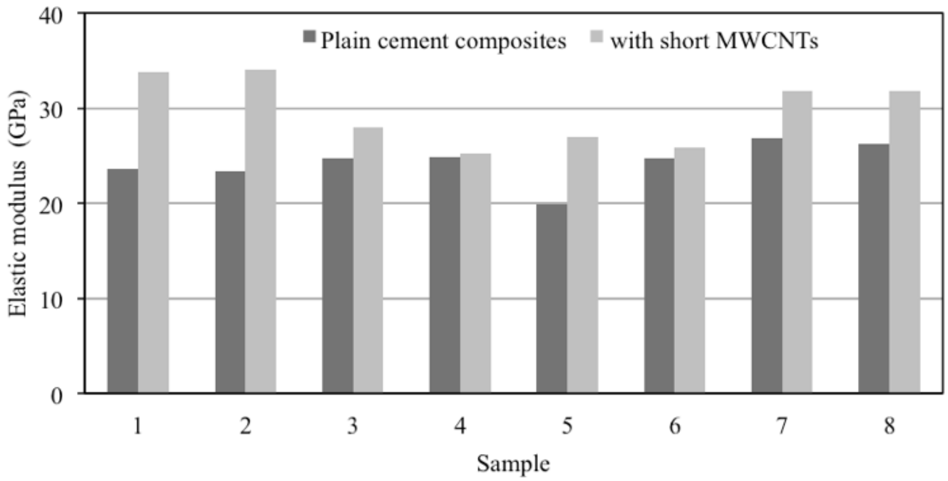

Fig. 4: Elastic modulus for 8 different samples

Since different materials were used for the nanoindentation testing, the elastic modulus results may differ from research to study. Table 4 shows the testing range for cement pastes that contain and do not contain short MWCNTs. Testing the log-converted elastic modulus data using the paired non-parametric test and paired p-tests at a 5% level confirmed the equal variance assumption for all eight samples. The test's p-value was found to be less than the alpha level (= 0.05). The implication is that there was insufficient data to establish whether the mean was consistently less than or equal to zero for both populations. The results support the alternative theory that shorter MWCNT composites have higher elastic modulus values than those without them.

Table 4: Standard Deviation (SD) of nanoindentation tests

Composites	Specimen 1	Specimen 2	Specime n 3	Specimen 4	Specime n 5	Specimen 6	Specime n 7	Specime n 8
Plain cement paste	6.16	0.53	2.89	3.20	2.53	2.41	3.09	3.12
With short MWCNTs	0.62	3.14	1.62	1.85	1.67	2.49	2.62	2.32

The load-displacement curves for cement pastes with and without short MWCNTs are shown in Figures 5 and 6, respectively. It is clear that short MWCNT-containing cement paste displaces less than conventional cement paste. For the same 1mN load, the largest displacement in plain cement composites is around 513 nm (Fig. 5), while the highest displacement in pastes with short MWCNTs is around 200 nm (Fig. 6). Short MWCNT cement paste is also dimensionally stable than regular cement paste, according to this study. As previously observed, the high-density CSH gel region was more noticeable than the low-density CSH gel when short MWCNTs were incorporated. The displacement values are therefore inversely correlated with the volume fractions of the low- and high-density CSH gels.

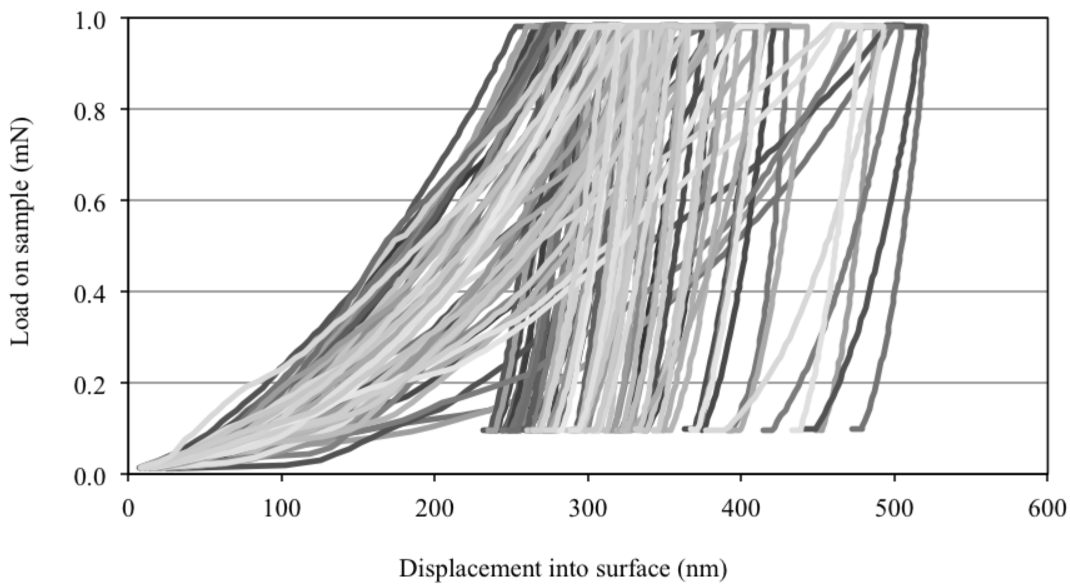

Fig. 5: Load vs. displacement curves for plain cement paste

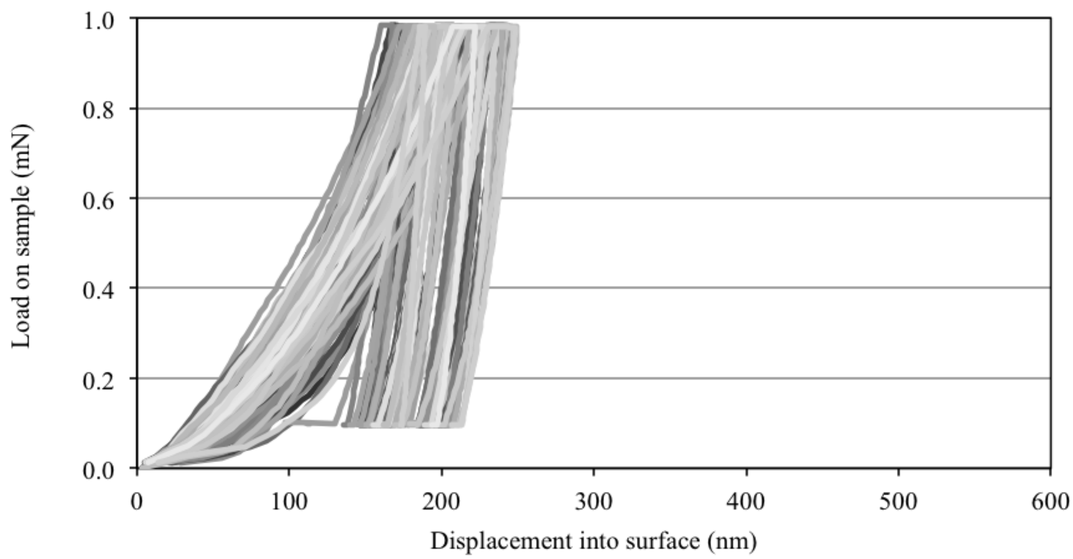

Fig. 6: Load vs. displacement curves for cement paste with short MWCNTs

3.2 Nano-scratching

The lateral force as a function of scratch length is shown in Figure 7. The lateral force required to dislodge a scratch length of 100m in normal cement paste increases consistently from roughly 0 to 15.5 mN.

Along the same 100 µm scratch length, the lateral force needed to remove cement paste augmented with short MWCNTs increases from 0 to 15.5 mN. However, there are small differences in the lateral force as well as the force necessary to dislocate the material highlighted by circles in Fig. 7. These oscillations could have been brought on by the tiny MWCNTs that were present in the cement matrix.

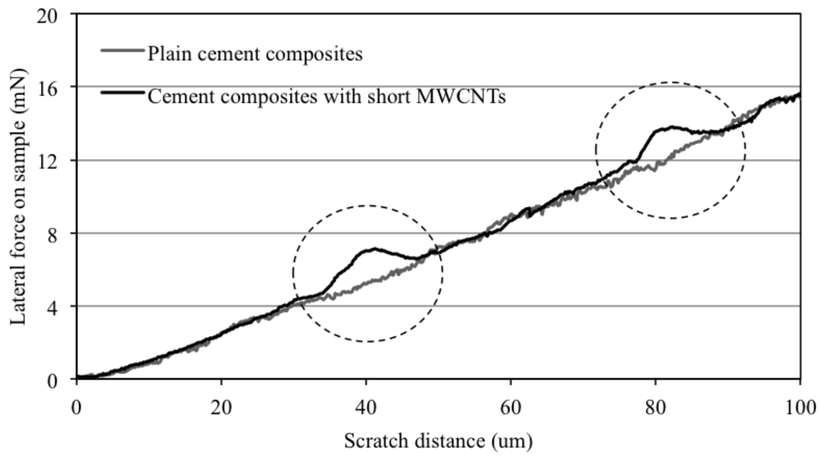

Fig. 7: Lateral force on the sample vs scratch distance

Figures 8 and 9 illustrate the pre-scan, scratch, and post-scan scratch profiles for regular cement paste and regular cement paste with short MWCNTs, respectively. The line graph at the bottom of Figures 8 and 9 with the scratch profile has drawn the most attention in this study. At all spots along the scratch profile, the indenter penetrates the scratch below the surface, implying that the normal load (50 mN) delivered by the indenter tip is sufficient to pierce the surface. As the cement pastes contain pores, CSH gel, and CH, all of which have different stiffness values, the penetration depths vary across the length of the scratch. The findings of Xu and Yao (2011) are consistent with this penetration depth trend.

As shown in Figures 8 and 9, the indenter penetrated deeper into the typical cement paste surface than the paste containing short MWCNTs. The short MWCNT paste's deepest penetration is less than 2000 nm, but the ordinary cement paste's deepest penetration is larger than 2000 nm. The material's mechanical response is reflected in the penetration depth, and a shallow penetration indicates a hard composition. As a result, short MWCNTs make it more difficult to permeate the substance than ordinary cement paste. However, further information on the occurrence of CH and clinker is needed before a firm conclusion can be reached.

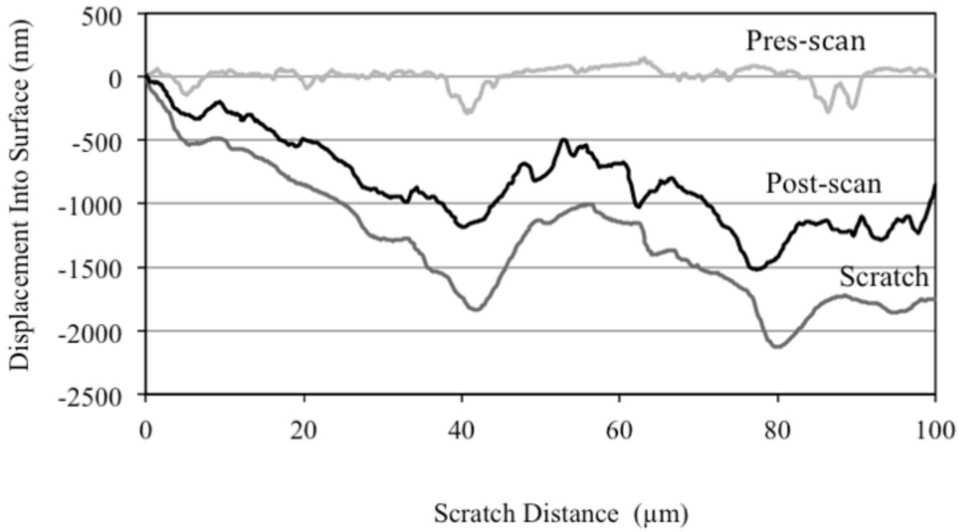

Fig. 8: Penetration depth vs scratch distance (plain cement paste)

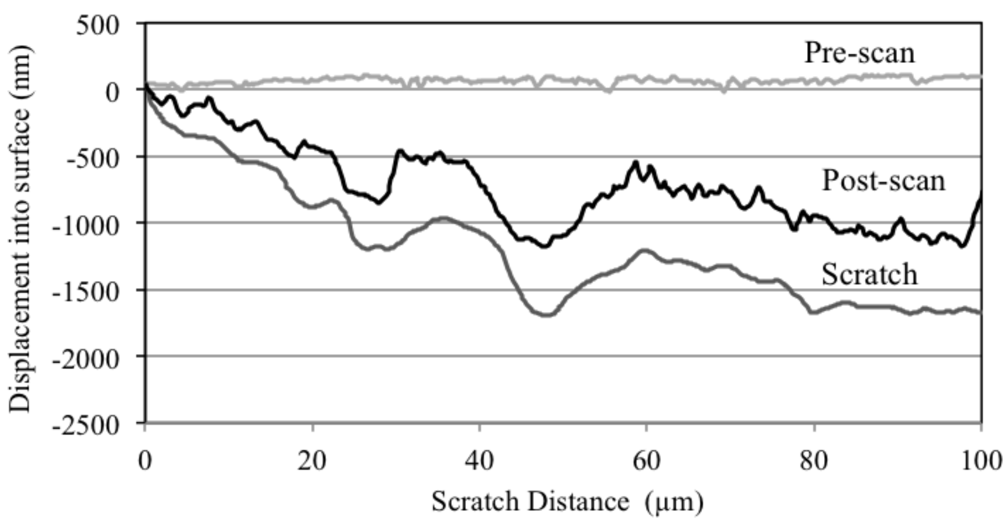

Fig. 9: Penetration depth vs scratch distance (cement paste with short MWCNTs)

The coefficient of friction is the measure of the relationship between the lateral force applied by the indentation tip and the normal force necessary to alter a material's surface (COF). The COF (three scratches) for cement paste with and without short MWCNTs as a function of scratch length is shown in Figures 10 and 11. The COF range for typical cement paste is 0.10 to 0.32. The rough surfaces of the samples could explain such discrepancies. The data indicate that the short MWCNT cement paste has COF values that are slightly higher than those of the traditional cement paste. This is expected given that short MWCNT cement pastes have lesser penetration depths than regular cement paste. The term COF, or scratch resistance, refers to the relationship between an increase in normal force and an increase in lateral force. This shows that the material had to be pierced with more lateral effort.

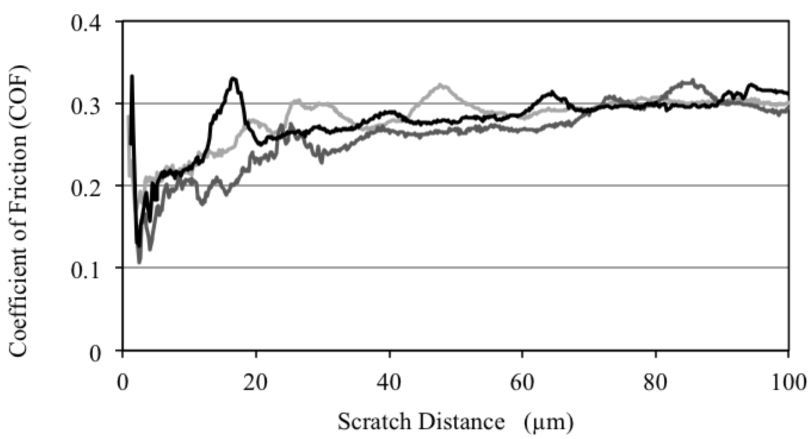

Fig. 10: Coefficient of friction for plain cement paste

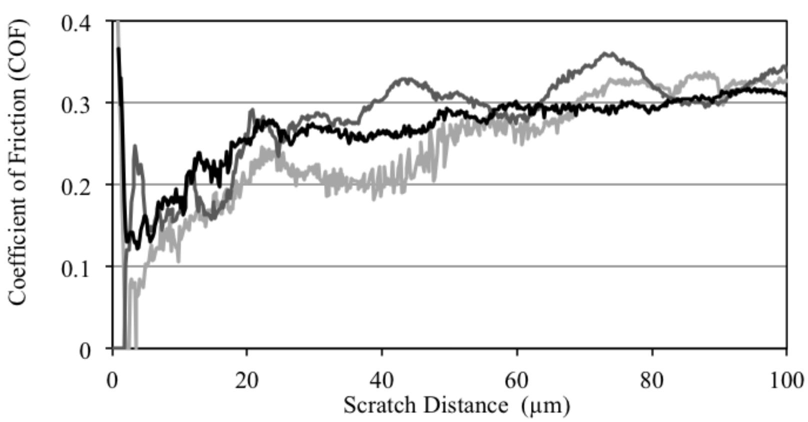

Fig. 11: Coefficient of friction for cement paste with short MWCNTs

Figure 12 shows a SEM image of cement paste with short MWCNTs. The short MWCNTs are visible bridging the cement mix's fractures. The effect of introducing short MWCNTs in the cement paste on their flexural strength is seen in Figure 13. Cement paste with short MWCNTs demonstrated better flexural strength than regular cement paste at all ages. The reason is the chemical interaction between carboxylic acid groups on the surface of carbon nanotubes and hydration products (Liew et al., 2016; Lu et al., 2015; Kim et al., 2019).

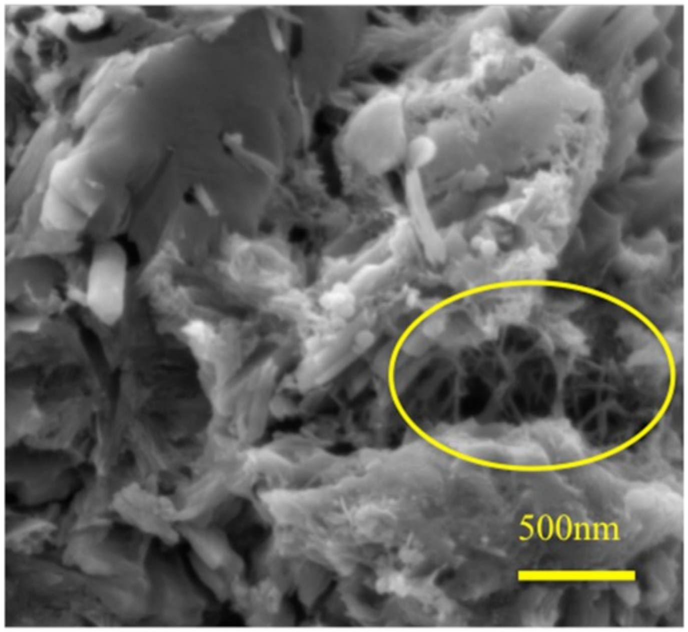

Fig. 12: Cracks bridging by short MWCNTs

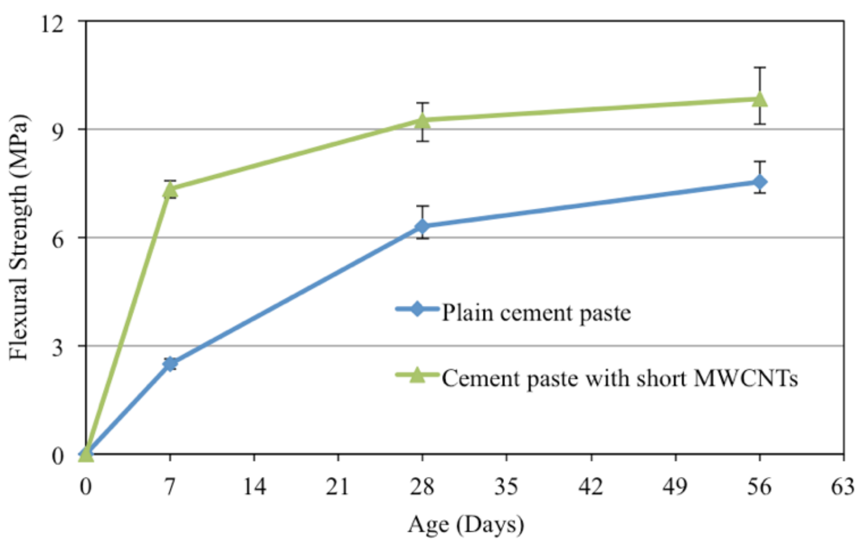

Fig. 13: Flexural strength of cement paste with and without MWCNTs

4. Conclusions

In this work, nanoindentation and nanoscratch techniques were used to assess the nanoscaled behaviour of cement paste reinforced with 0.30 percent (by weight of cement) short MWCNTs. The results of the experiment lead to the following conclusions:

- The high-density CSH gel area becomes more evident when short MWCNTs are introduced to cement pastes, and cement pastes with short MWCNTs have higher elastic modulus values than pastes without them.
- Both the standard cement paste and the cement paste with short MWCNTs require the same amount of lateral force to displace.
- When compared to the paste containing short MWCNTs, the indenter penetrates the plain cement paste surface less. This suggests that the material is more difficult to penetrate when short MWCNTs are present.
- In comparison to normal cement paste, the coefficient of friction of cement pastes with short MWCNTs is higher.

References:

- Chen, S. J., Collins, F. G., Macleod, A. J. N., Pan, Z., Duan, W. H., & Wang, C. M. (2011). Carbon nanotube-cement composites: A retrospect. The IES Journal Part A: Civil and Structural Engineering, 4(4), 254-265.
- Savastano, J. H., Warden, P. G., & Coutts, R. S. P. (2005). Microstructure and mechanical properties of waste fibre-cement composites. Cement and Concrete Composites, 27(5), 583–592.
- Fischer, G., & Li, V. C. (2007). Effect of fiber reinforcement on the response of structural members. Engineering Fracture Mechanics, 74(1–2), 258–272.
- Wang, C., Li, K. Z., Li, H. J., Jiao, G. S., Lu, J., & Hou, D. S. (2008). Effect of carbon fiber dispersion on the mechanical properties of carbon fiber-reinforced cement-based composites. Materials Science and Engineering: A, 487(1–2), 52–57.
- Lau, K. T., & Hui, D. (2002). The revolutionary creation of new advanced materials—carbon nanotube. Composites Part B, 33, 263–277.
- Chen, W. X., Tu, J. P., Wang, L. Y., Gan, H. Y., Xu, Z. D., & Zhang, X. B. (2003). Tribological application of carbon nanotubes in a metal-based composite coating and composites. Carbon, 41, 215–222.
- Lee, H., Mall, S., He, P., Shi, D., Narasimhadevara, S., Yun, Y. H., Shanov, V., & Schulz, M. J. (2007). Characterization of carbon nanotube/nanofiber-reinforced polymer composites using an instrumented indentation technique. Composites Part B, 38, 58–65.

- Wei, T., Fan, Z., Luo, G., & Wei, F. (2008). A new structure for multi-walled carbon nanotubes reinforced alumina nano-composite with high strength and toughness. Materials Letters, 2, 641–644.
- Zhu, Y. F., Shi, L., Liang, J., Hui, D., & Lau, K. T. (2008). Synthesis of zirconia nanoparticles on carbon nanotubes and their potential for enhancing the fracture toughness of alumina ceramics. Composites Part B, 39, 1136–1141.
- Esawia, A. M. K., Morsi, K., Sayed, A., Gawad, A. A., & Borah, P. (2009). Fabrication and properties of dispersed carbon nanotube–aluminum composites. Materials Science and Engineering: A, 508(1), 167–173.
- Wang, B., Han, Y., & Zhang, T. (2014). Reinforcement of surface-modified multi-walled carbon nanotubes on cement-based composites. Advances in Cement Research, 26(2), 77-84.
- Sahranavard, S., Kazemi, H. H., & Abbasi, S. (2014). Effect of multi-walled carbon nanotubes on mechanical properties of high-performance mortar. Magazine of Concrete Research, 66(18), 948-954.
- Li, Q., Liu, J., & Xu, S. (2015). Progress in research on carbon nanotubes reinforced cementitious composites. Advances in Materials Science and Engineering, 2015, 1-16.
- Gillani, S. S., Khitab, A., Ahmad, S., Khushnood, R. A., Ferro, G. A., Kazmi, S. M. S., Qureshi, L. A., & Restuccia, L. (2017). Improving the mechanical performance of cement composites by carbon nanotubes addition. Procedia Structural Integrity, 3, 11-17.
- Abu Al-Rub, R. K., Ashour, A. I., & Tyson, B. M. (2012). On the aspect ratio effect of multi-walled carbon nanotube reinforcements on the mechanical properties of cementitious nanocomposites. Construction and Building Materials, 35, 647-655.
- Hawreen, A., & Bogas, J. A. (2019). Creep, shrinkage and mechanical properties of concrete reinforced with different types of carbon nanotubes. Construction and Building Materials, 198, 70-81.
- Wang, J., Dong, S., Ashour, A. F., Wang, X., & Han, B. (2020). Dynamic mechanical properties of cementitious composites with carbon nanotubes. Materials Today Communications, 22, 100722.
- Yoo, D. Y., You, I., & Lee, S. J. (2018). Electrical and piezoresistive sensing capacities of cement paste with multi-walled carbon nanotubes. Archives of Civil and Mechanical Engineering, 18, 371-384.
- Li, Y., Li, H., Wang, Z., & Jin, C. (2020). Effect and mechanism analysis of functionalized multi-walled carbon nanotubes (MWCNTs) on C-S-H gel. Cement and Concrete Research, 128, 105955.
- Cui, X., Han, B., Zheng, Q., Yu, X., Dong, S., Zhang, L., & Ou, J. (2017). Mechanical properties and reinforcing mechanisms of cementitious composites with different types of multiwalled carbon nanotubes. Composites Part A: Applied Science and Manufacturing, 103, 131-147.
- Hawreen, A., Bogas, J. A., & Dias, A. P. S. (2018). On the mechanical and shrinkage behavior of cement mortars reinforced with carbon nanotubes. Construction and Building Materials, 168, 459-470.
- Arrechea, S., Guerrero-Gutiérrez, E. M. A. L., Cardona, J., Posadas, R., Callejas, K., Torres, S., Diaz, R., Barrientos, C., & Garcia, E. (2020). Effect of additions of

multiwall carbon nanotubes (MWCNT, MWCNT-COOH and MWCNT-Thiazol) in mechanical compression properties of a cement-based material. Materialia, 11, 100739.

- Mondal, P., Shah, S. P., & Marks, L. D. (2007). A reliable technique to determine the local mechanical properties at the nanoscale for cementitious materials. Cement and Concrete Research, 37(10), 1440–1444.
- Sorelli, L., Constantinides, G., Ulm, F. J., & Toutlemonde, F. (2008). The nanomechanical signature of ultra-high-performance concrete by statistical nanoindentation techniques. Cement and Concrete Research, 38(12), 1447–1456.
- Vandamme, M., Ulm, F. J., & Fonollosa, P. (2010). Nanogranular packing of C–S–H at sub-stoichiometric conditions. Cement and Concrete Research, 40(1), 14–26.
- Davydov, D., Jirásek, M., & Kopecký, L. (2011). Critical aspects of nanoindentation technique in application to hardened cement paste. Cement and Concrete Research, 41(1), 20–29.
- Adams, M. J., Allan, A., Briscoe, B. J., Doyle, P. J., Gorman, D. M., & Johnson, S. A. (2001). An experimental study of the nanoscratch behavior of poly(methyl methacrylate). Wear, 250, 1579–1583.
- Shen, W. D., Mi, L., & Jiang, B. (2006). Characterization of mar/scratch resistance of coatings with a nanoindenter and a scanning probe microscope. Tribology International, 39(2), 146–158.
- Graça, S., Colaço, R., & Vilar, R. (2008). Micro-to-nano indentation and scratch hardness in the Ni–Co system: depth dependence and implications for tribological behavior. Tribology Letters, 31(3), 177–185.
- Wang, B., Han, Y., & Liu, S. (2013). Effect of highly dispersed carbon nanotube on the flexural toughness of cement-based composites. Construction and Building Materials, 46, 8-12.
- Kumar, S., Kolay, P., Malla, S., & Mishra, S. (2012). Effect of multi-walled carbon nanotubes on mechanical strength of cement paste. Journal of Materials in Civil Engineering, 24(1), 84–91.
- AS 3972 (2010): General Purpose and Blended Cements. Standard Australia.
- Yazdanbakhsh, A., Grasley, Z., Tyson, B., & Abu Al-Rub, R. (2009). Carbon nanofibers and nanotubes in cementitious materials: Some issues on dispersion and interfacial bond. ACI Special Publication, 267, 21–34.
- Fischer-Cripps, A. C. (2006). Critical review of analysis and interpretation of nanoindentation test data. Surface and Coatings Technology, 200(14-15), 4153-4165.
- Acker, P. (2001). Micromechanical analysis of creep and shrinkage mechanisms. In Creep, shrinkage and durability mechanics of concrete and other quasi-brittle materials. Elsevier, Cambridge: 201-211.
- Velez, K., Maximilien, S., Damidot, D., Fantozzi, G., & Sorrentino, F. (2001). Determination by nanoindentation of elastic modulus and hardness of pure constituents of Portland cement clinker. Cement and Concrete Research, 31(4), 555–561.
- Constantinides, G., & Ulm, F.-J. (2004). The effect of two types of C–S–H on the elasticity of cement-based materials: results from nanoindentation and micromechanical modelling. Cement and Concrete Research, 34, 67–80.

- Xu, J., & Yao, W. (2011). Nano-scratch as a new tool for assessing the nano-tribological behaviour of cement composite. Materials and Structures, 44, 1703–1711.
- Kim, G. M., Nam, I. W., Yang, B., Yoon, H. N., Lee, H. K., & Park, S. (2019). Carbon nanotube (CNT) incorporated cementitious composites for functional construction materials: The state of the art. Composites Structures, 227, 111244.
- Liew, K. M., Kai, M. F., & Zhang, L. W. (2016). Carbon nanotube reinforced cementitious composites: An overview. Composites Applied Science and Manufacturing, 91, 301-323.
- Lu, Z., Hou, D., Meng, L., Sun, G., Lu, C., & Li, Z. (2015). Mechanism of cement paste reinforced by graphene oxide/carbon nanotubes composites with enhanced mechanical properties. 5, 100598-100605.